

Original article

# Differences in Frame Geometry Between Balloon-expandable and Self-expanding Transcatheter Heart Valves and Association With Aortic Regurgitation<sup>☆</sup>



Ramón Rodríguez-Olivares,<sup>a</sup> Zouhair Rahhab,<sup>a</sup> Nahid El Faquir,<sup>a</sup> Ben Ren,<sup>a</sup> Marcel Geleijnse,<sup>a</sup> Nico Bruining,<sup>a</sup> Nicolas M. van Mieghem,<sup>a</sup> Carl Schultz,<sup>b</sup> Guenter Lauritsch,<sup>c</sup> and Peter P.T. de Jaegere<sup>a,\*</sup>

<sup>a</sup> Department of Cardiology, Erasmus Medical Center, Rotterdam, The Netherlands

<sup>b</sup> Department of Cardiology, Royal Perth Hospital Campus, School of Medicine and Pharmacology, University of Western Australia, Crawley, Australia

<sup>c</sup> Siemens Healthcare GmbH, Forchheim, Germany

Article history:

Received 16 April 2015

Accepted 3 August 2015

Available online 28 November 2015

Keywords:

Aortic valve stenosis

Transcatheter aortic valve replacement

Rotational angiography

ABSTRACT

**Introduction and objectives:** Patient- and procedure-related factors are known to be associated with aortic regurgitation after transcatheter aortic valve implantation. Nevertheless, this entity may also be caused by a specific device-host interaction due to the biomechanical properties of the valves, independently of clinical factors. We sought to elucidate the role of frame geometry in the occurrence of aortic regurgitation after Medtronic CoreValve and Edwards SAPIEN valve implantation.

**Methods:** We conducted an observational study encompassing 134 patients undergoing transcatheter aortic valve implantation with the Medtronic CoreValve and Edwards SAPIEN valve. Frame analysis was performed at 3 predefined levels of both valves by rotational angiography using dedicated motion compensation software. A distinction was made between patients with no-to-mild and moderate-to-severe aortic regurgitation by echocardiography.

**Results:** Baseline characteristics were similar between the 2 valves. Despite greater use of predilation in the CoreValve (95.2% vs 82.0%;  $P = .012$ ), more oversizing (perimeter,  $114 \pm 7\%$  vs  $103 \pm 7\%$ ;  $P < .001$ ), and the same depth of implantation (noncoronary sinus,  $7 \pm 4$  vs  $8 \pm 2$  mm; left coronary sinus,  $8 \pm 4$  vs  $8 \pm 2$  mm), it was less expanded and more eccentric than the Edwards SAPIEN ( $83 \pm 7\%$  vs  $92 \pm 4\%$ ;  $P < .001$  and  $82 \pm 8\%$  vs  $95 \pm 3\%$ ;  $P < .001$ , respectively) and when eccentricity was adjusted for the patient's annulus eccentricity ( $4 \pm 13\%$  vs  $21 \pm 11\%$ ;  $P < .001$ ). Eccentricity and adjusted eccentricity were associated with moderate-to-severe aortic regurgitation.

**Conclusions:** Independently of patient- and procedure-related factors, there is a device-specific device-host interaction that explains aortic regurgitation after transcatheter aortic valve implantation.

© 2015 Sociedad Española de Cardiología. Published by Elsevier España, S.L.U. All rights reserved.

## Diferencias en geometría entre válvulas percutáneas expandibles con balón y autoexpandibles y su relación con la insuficiencia aórtica

RESUMEN

**Introducción y objetivos:** Se sabe que los factores relacionados con el paciente y con la intervención se asocian con insuficiencia aórtica después de un implante percutáneo de válvula aórtica. No obstante, también puede causarla una interacción específica entre el dispositivo y el huésped como consecuencia de las propiedades biomecánicas de las válvulas, con independencia de los factores clínicos. El objetivo de este estudio es esclarecer el papel de la geometría de la válvula en la aparición de insuficiencia aórtica después del implante de las válvulas Medtronic CoreValve<sup>®</sup> y Edwards SAPIEN<sup>®</sup>.

**Métodos:** Se llevó a cabo un estudio observacional que incluyó a 134 pacientes tratados con implante percutáneo de válvula aórtica empleando las válvulas Medtronic CoreValve<sup>®</sup> y Edwards SAPIEN<sup>®</sup>. El análisis geométrico se realizó en tres niveles predefinidos de ambas válvulas mediante angiografía rotacional con compensación de movimiento usando un programa informático específicamente desarrollado para este fin. Se estableció una distinción entre los pacientes con insuficiencia aórtica nula o leve y los pacientes con insuficiencia aórtica moderada o grave según la ecocardiografía.

Palabras clave:

Estenosis valvular aórtica

Sustitución percutánea de válvula aórtica

Angiografía rotacional

<sup>☆</sup> The concepts and information presented in this paper are based on research and are not commercially available. The product names and brands referred to are the property of their respective trademark holders.

\* Corresponding author: Thorax Center, Department of Cardiology, Erasmus MC, s-Gravendijkwal 230, 3015 CE Rotterdam, The Netherlands.  
E-mail address: [p.dejaegere@erasmusmc.nl](mailto:p.dejaegere@erasmusmc.nl) (P.P.T. de Jaegere).

**Resultados:** Las características basales eran similares con ambas válvulas. A pesar del mayor uso de predilatación en el grupo de CoreValve® (el 95,2 frente al 82,0%;  $p = 0,012$ ), el mayor exceso de tamaño de prótesis/anillo aórtico (perímetro, el  $114 \pm 7\%$  frente al  $103 \pm 7\%$ ;  $p < 0,001$ ) y la misma profundidad de implante (seno no coronario,  $7 \pm 4$  frente a  $8 \pm 2$  mm; seno coronario izquierdo,  $8 \pm 4$  frente a  $8 \pm 2$  mm), esta válvula tuvo menos expansión (el  $83 \pm 7\%$  frente al  $92 \pm 4\%$ ;  $p < 0,001$ ) y fue más excéntrica (el  $82 \pm 8\%$  frente al  $95 \pm 3\%$ ;  $p < 0,001$ ) que la válvula Edwards SAPIEN®, también tras introducir un ajuste de la excentricidad respecto a la excentricidad del anillo valvular del paciente (el  $4 \pm 13\%$  frente al  $21 \pm 11\%$ ;  $p < 0,001$ ). La excentricidad y la excentricidad ajustada se asociaron con insuficiencia aórtica moderada o grave.

**Conclusiones:** Independientemente de los factores relacionados con el paciente y con la intervención, existe una interacción entre dispositivo y huésped que es específica del dispositivo y explica la insuficiencia aórtica existente después de un implante percutáneo de válvula aórtica.

© 2015 Sociedad Española de Cardiología. Publicado por Elsevier España, S.L.U. Todos los derechos reservados.

### Abbreviations

AR: aortic regurgitation  
 ESV: Edwards SAPIEN valve  
 MCS: Medtronic CoreValve system  
 MSCT: multislice computed tomography  
 TAVI: transcatheter aortic valve implantation

## INTRODUCTION

Transcatheter aortic valve implantation (TAVI) is increasingly used for patients with severe aortic stenosis at high risk for surgical valve replacement and has been shown to be safe and effective compared with aortic valve replacement in such patients.<sup>1–5</sup> Nevertheless, aortic regurgitation (AR) often occurs and is usually paravalvular. It is more frequent after the implantation of the self-expanding Medtronic CoreValve System (MCS) than the balloon-expandable Edwards SAPIEN valve (ESV).<sup>6–8</sup>

Patient- and procedure-related variables such as the amount and distribution of aortic root calcification, annular dimensions, the depth of implantation, and sizing have been identified as determinants of AR post-TAVI.<sup>9,10</sup> Nevertheless, AR may also stem from a specific device-host interaction due to the intrinsic biomechanical properties of valves that in turn may affect frame geometry and the degree of expansion contributing to AR. There is evidence from multislice computed tomography (MSCT) analysis in selected patients that noncircular expansion and malapposition is more frequent after MCS than ESV valve implantation.<sup>11–14</sup> To further elucidate the role of frame geometry and degree of expansion in relation to established patient- and procedure-related variables associated with AR, we incorporated rotational angiography with dedicated motion compensation 3-dimensional image reconstruction immediately after TAVI.<sup>15</sup> The objective of this study was to assess and compare the geometric findings by rotational angiography between the MCS and ESV valve and its association with AR.

## METHODS

### Patients

This was an prospective observational study with a study population of 150 consecutive patients with symptomatic severe

aortic stenosis who underwent TAVI with the MCS or ESV and who underwent rotational angiography.<sup>15</sup> Only patients with a single valve implantation (ie, patients with a valve-in-valve procedure were excluded) in a native aortic valve (ie, patients with failed bioprosthesis were excluded) and sufficient image quality for frame assessment (grade 1, 2 or 3) were included using the following score: grade 1, excellent image quality (struts visible without artifacts); grade 2, struts clearly visible, distinction between struts and artifacts possible; grade 3, struts visible but in some regions the distinction between struts and artifacts cannot be made; grade 4, degraded (struts are blurred and distorted), and grade 5, strongly degraded (struts and artefacts cannot be distinguished) (Figure 1). A total of 16 patients (MCS 14, ESV 2) were excluded from the analysis because of image quality grade 4 (8 patients) and 5 (8 patients). Therefore, the total study population was 134 (MCS 84, ESV 50).

All patients underwent TAVI under general anesthesia via the femoral or subclavian artery or left ventricular apex after heart-team discussion. The MSCT was used for sizing in all patients except 9.<sup>16</sup> Patients were first seen at the outpatient clinic and gave written informed consent for anonymized prospective data collection for clinical research purpose (TAVI Care and Cure project, MEC-2014-277).

### Rotational Angiography, 3-dimensional Reconstruction and Frame Analysis

Rotational angiography was performed immediately after TAVI using the Artis zee angiographic C-arm system (Siemens Healthcare GmbH; Forchheim, Germany) with a  $20 \times 20$  cm detector and isotropic pixel length of  $180 \mu\text{m}$ . A total of 133 images were acquired in 5 seconds along a  $198^\circ$  arc ( $99^\circ$  right anterior oblique to  $99^\circ$  left anterior oblique view) during breath hold at a detector entrance dose of  $0.36 \mu\text{m}$  per frame.

#### Three-dimensional Reconstruction

From the projection images, a motion-compensated 3-dimensional image was reconstructed with prototype software (Siemens Healthcare GmbH) with a matrix of 256 and  $0.5 \text{ mm}^3$  voxel size using a standard operating procedure.<sup>15</sup> In summary, an electrocardiogram-gated reconstruction was made using the end-diastolic phase at 75% of the cardiac cycle since at that moment there is theoretically less motion. The electrocardiogram-gated reconstruction was used as a reference image for estimating

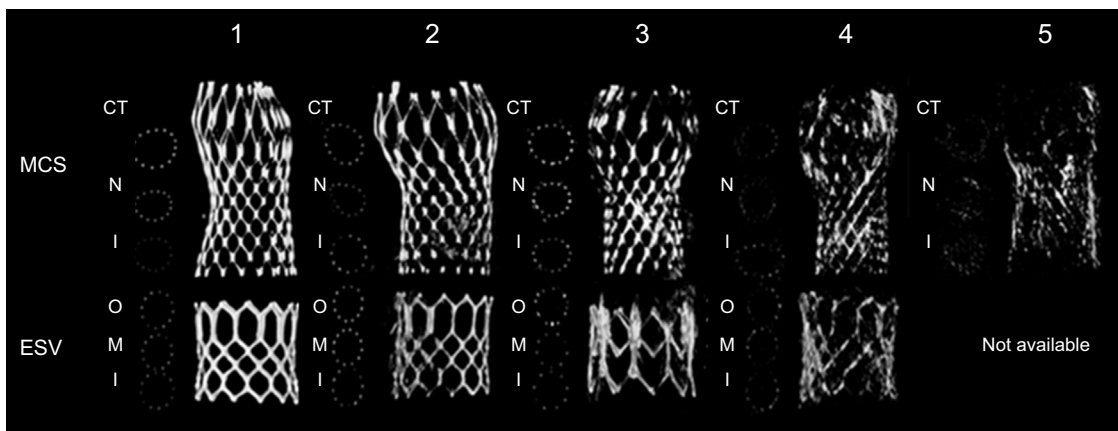


**Figure 1.** Image quality of rotational angiography; grade 1 (best quality) to grade 5 (worst). CT, central coaptation of the leaflets; ESV, Edwards SAPIEN valve; I, inflow; M, mid segment; MCS, Medtronic CoreValve system; N, nadir; O, outflow.

cardiac motion. The estimated motion was compensated in a final reconstruction step. The total process took approximately 5 minutes. The 3-dimensional reconstruction of the frame was then processed (eg, cropping) before analysis. Cross-sectional images were used for frame analysis.

*Frame Analysis*

Frame analysis was performed at 3 predefined levels of both valves. The dimensions of the MCS were measured at the inflow (0 mm), nadir of leaflets (12 mm from inflow), and central coaptation (24 mm from inflow), as previously described.<sup>13</sup> The dimensions of the ESV were measured at the inflow (0 mm), mid segment (at 50% for XT, at the 3rd cross section for S3) (Figure 2), and outflow (top). At each of these levels, the minimum diameter ( $D_{min}$ ), maximum diameter ( $D_{max}$ ), area and perimeter were manually measured using the center point of the strut or struts (Figure 2).

Valve sizing was defined by dividing the nominal valve size by the MSCT-derived annulus measures ( $D_{min}$ ,  $D_{max}$ ,  $D_{mean}$  and perimeter)  $\times 100$  (%). The degree of frame expansion was calculated by dividing the measured perimeter by the nominal perimeter of that level ( $perimeter_{frame-measured}/perimeter_{frame-nominal}$ ), as well as by relating the degree of expansion to the

annulus perimeter (ie, adjusted degree of expansion) by calculating:  $perimeter_{valve-measured}/perimeter_{annulus}$ . For the MCS valve, the following nominal perimeters were used: inflow, 72.3, 81.7, 91.1 and 97.4 mm for 23, 26, 29 and 31 mm, respectively; nadir, 64.4, 75.4, 79.8 and 83.9 mm for 23, 26, 29 and 31 mm, respectively, and central coaptation, 68.8, 69.1, 72.6 and 76.3 mm for 23, 26, 29 and 31 mm, respectively (source: Medtronic Inc.; Minneapolis, United States). For the ESV, the calculated nominal perimeter of the inflow (ie,  $\pi \times D_{nominal}$ ) was used for all levels given the tubular shape of the ESV. The eccentricity of the frame was calculated by  $D_{frame-min}/D_{frame-max}$  at all levels. The eccentricity at the nadir (MCS) and mid segment (ESV) was adjusted to the eccentricity of the native valve using the following equation: (eccentricity nadir or mid segment - eccentricity native annulus/eccentricity native annulus)  $\times 100$ . This was done since this part of the frame is closer to the patients' native annulus than the other parts of the frame.

**Assessment of Aortic Regurgitation**

Contrast angiography and Doppler echocardiography were used to assess AR immediately after TAVI and at discharge. With respect to contrast angiography, AR severity was defined using Sellers' classification (0 = none, 1 = mild, 2 = moderate, 3 = moderate to severe, and 4 = severe).<sup>17</sup> For that purpose, a predefined angiography

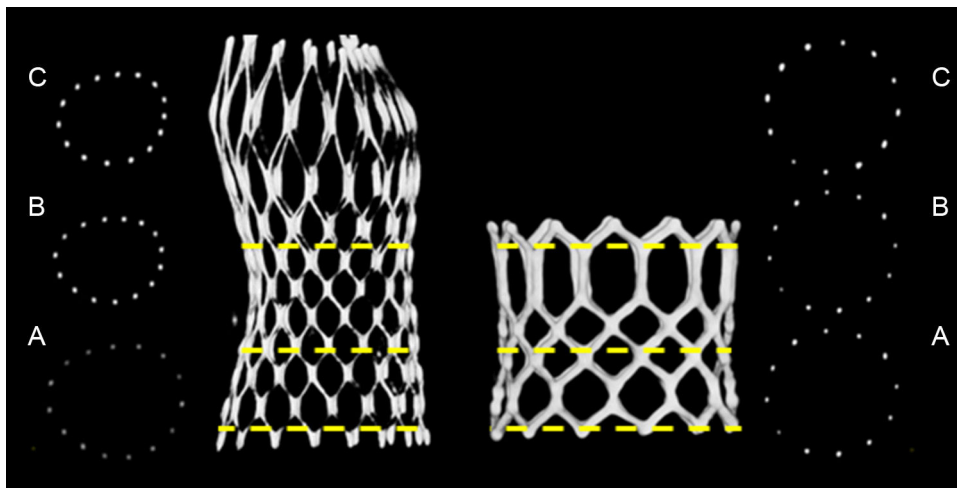


**Figure 2.** Cross-sectional view at the 3 levels of interest of the self-expanding Medtronic CoreValve and Edwards SAPIEN frame. A: inflow, B: nadir/mid segment; C: coaptation/outflow.

protocol was used that consisted of the injection of 20 ml undiluted iodixanol (Visipaque™) at a flow rate of 20 ml/s via a 6-Fr pigtail that was positioned just above the bioprosthetic leaflets. Cine runs were recorded at a speed of 30 frames/s. Two observers scored the angiograms independently from each another. If there was a discrepancy, consensus was reached by including a third observer. The intra- and interobserver variability for the assessment of AR post-TAVI according to Sellers' classification were  $k = 0.70$  and  $k = 0.78$ , respectively. A distinction was made between patients with Sellers' grade 0-1 and those with Sellers' grade 2-4.

Transthoracic Doppler echocardiography was performed before discharge. The AR severity was defined by the circumferential extent of the Doppler signal at the inflow of the MCS frame in the parasternal short axis view using the VARC-2 (Valve Academic Research Consortium-2) criteria.<sup>18</sup> Echocardiography of sufficient quality to assess AR was available in 119 out of the 134 patients (89%). A distinction was made between patients with no AR and

mild AR ( $< 10\%$ ) and those with moderate and severe AR ( $10\%$  to  $29\%$  and  $\geq 30\%$ ).

### Statistical Analysis

Categorical variables are presented as frequencies and percentages and compared with the Pearson chi-square test. The normality of the continuous variables distributions was assessed using the Kolmogorov-Smirnov test and, since all the variables studied were (nearly) normally-distributed results, are presented as means  $\pm$  standard deviation and compared with the Student *t* test. Interobserver variability was calculated using intraclass correlation (Table 1 of the supplementary material). Statistical analyses were performed using SPSS software version 21.0 (IBM SPSS Statistics for Windows, Version 21.0; Armonk, New York, United States).

**Table 1**  
Baseline Characteristics

	Entire cohort (n = 134)	MCS (n = 84)	ESV (n = 50)	P
Age, y	82 $\pm$ 9	80 $\pm$ 9	78 $\pm$ 10	.141
Male	78 (58.2)	47 (56.0)	31 (62.0)	.492
Height, cm	169 $\pm$ 9	168 $\pm$ 10	170 $\pm$ 9	.253
Weight, kg	76 $\pm$ 15	74 $\pm$ 14	80 $\pm$ 15	.020
Body mass index	26 $\pm$ 5	26 $\pm$ 5	28 $\pm$ 5	.069
Body surface area, m <sup>2</sup>	1.9 $\pm$ 0.2	1.8 $\pm$ 0.2	1.9 $\pm$ 0.2	.044
NYHA functional class $\geq$ III	93 (69.4)	59 (72.8)	34 (72.3)	.951
Previous CVA	30 (22.4)	22 (26.2)	8 (16.0)	.171
Previous MI	31 (23.1)	20 (23.8)	11 (22.0)	.810
Previous CABG	31 (23.1)	21 (25.0)	10 (20.0)	.507
Previous PCI	35 (26.1)	23 (27.4)	12 (24.0)	.667
Diabetes mellitus	30 (22.4)	17 (20.2)	13 (26.0)	.439
Hypertension	103 (76.9)	61 (72.6)	42 (84.0)	.131
Peripheral vascular disease	36 (26.9)	19 (22.6)	17 (34.0)	.151
Pulmonary hypertension	11 (8.2)	5 (6.0)	6 (12.0)	.217
Severe pulmonary hypertension	4 (3.0)	1 (1.2)	3 (6.0)	.114
COPD	36 (26.9)	26 (31.0)	10 (20.0)	.167
Atrial fibrillation	35 (26.1)	21 (25.0)	14 (28.0)	.702
Permanent pacemaker	9 (6.7)	4 (4.8)	5 (10.0)	.241
Logistic EuroSCORE, %	17 $\pm$ 12	17 $\pm$ 11	16 $\pm$ 13	.678
<b>Echocardiography and cardiac catheterization</b>				
LVEF, %	54 $\pm$ 14	51 $\pm$ 14	50 $\pm$ 13	.864
Aortic valve area, cm <sup>2</sup>	0.70 $\pm$ 0.2	0.69 $\pm$ 0.2	0.74 $\pm$ 0.2	.182
Peak gradient, mmHg	68 $\pm$ 25	72 $\pm$ 27	72 $\pm$ 21	.993
Mitral regurgitation $\geq$ II	66 (49.3)	35 (41.7)	31 (64.6)	.011
AR baseline $\geq$ II	62 (46.3)	35 (41.7)	27 (57.4)	.083
AR index	25 $\pm$ 11	26 $\pm$ 12	24 $\pm$ 7	.498
<b>Multislice computed tomography</b>				
Minimal annulus diameter, mm	22 $\pm$ 2	22 $\pm$ 2	22 $\pm$ 2	.614
Maximal annulus diameter, mm	27 $\pm$ 3	27 $\pm$ 3	28 $\pm$ 3	.110
Mean annulus diameter, mm	25 $\pm$ 2	25 $\pm$ 2	25 $\pm$ 2	.239
Perimeter annulus, mm	79 $\pm$ 7	78 $\pm$ 7	81 $\pm$ 8	.049
Area annulus, mm <sup>2</sup>	469 $\pm$ 84	469 $\pm$ 83	488 $\pm$ 85	.203
Annulus eccentricity, %	80 $\pm$ 6	81 $\pm$ 6	79 $\pm$ 6	.240
Agatston score	3614 $\pm$ 2403	3349 $\pm$ 1922	4010 $\pm$ 2964	.150

AR, aortic regurgitation; CABG, coronary artery bypass; COPD, chronic obstructive pulmonary disease; CVA, cerebrovascular event; ESV, Edwards SAPIEN valve; LVEF, left ventricular ejection fraction; MCS, Medtronic CoreValve system; MI, myocardial infarction; NYHA, New York Heart Association; PCI, percutaneous coronary intervention. Data are expressed as no. (%) or mean  $\pm$  standard deviation

The main analysis consisted of the comparison of the geometry of the MCS and the ESV. The secondary analysis consisted of the assessment of the relationship between the geometry of the frame of both valves and AR. A distinction was made between (none or mild (< 10%) vs moderate or severe (10% to 29% and  $\geq$  30%) AR based on the short axis view of the echocardiography-Doppler examination before discharge (VARC-2 criteria).<sup>18</sup>

## RESULTS

The baseline clinical and procedural data of all patients and of those treated with the MCS or ESV valve are summarized in Tables 1 and 2. By univariable analysis, there were no differences

between patients treated with the MCS or ESV valve except for a lower body weight ( $74 \pm 14$  kg vs  $80 \pm 15$  kg;  $P = .02$ ), lower body surface area ( $1.8 \pm 0.2$  m<sup>2</sup> vs  $1.9 \pm 0.2$  m<sup>2</sup>;  $P = .044$ ), a lesser prevalence of mitral regurgitation  $\geq$  II at baseline (41.7% vs 64.6%;  $P = .021$ ), and smaller annulus perimeter ( $78 \pm 7$  mm vs  $81 \pm 8$  mm;  $P = .049$ ) in patients treated with the MCS valve.

From a procedural perspective, patients treated with the MCS valve more often underwent balloon predilatation than patients treated with the ESV valve (95.2% vs 82.0%;  $P = .012$ ), albeit with a smaller balloon in relation to the patient's annulus (mean balloon diameter/mean diameter annulus  $\times$  100 MCS vs ESV:  $91 \pm 7\%$  vs  $94 \pm 5\%$ ;  $P = .024$ ), and also received a larger valve relative to all MSCT-derived annulus measures compared with patients receiving the ESV (MCS vs ESV:  $D_{\min}$ ,  $130 \pm 10$  mm; vs  $121 \pm 8$  mm;  $P < .001$ ;

**Table 2**  
Procedural Details

	Entire cohort (n=134)	MCS (n=84)	ESV (n=50)	P
<b>Access</b>				
Transfemoral	129 (96.3)	82 (97.6)	47 (94.0)	
Transsubclavian	2 (1.5)	2 (2.4)	0 (0.0)	
Transapical	3 (2.2)	0 (0.0)	3 (6.0)	
<b>Prosthesis size</b>				
23 mm	8 (6.0)	1 (1.2)	7 (14.0)	
26 mm	46 (34.3)	20 (23.8)	26 (52.0)	
29 mm	72 (53.7)	55 (65.5)	17 (34.0)	
31 mm	8 (6.0)	8 (9.5)	0 (0.0)	
<b>Predilatation</b>				
Preimplantation balloon dilation	121 (90.3)	80 (95.2)	41 (82.0)	.012
Balloon nominal/mean annulus diameter $\times$ 100, %	92 $\pm$ 7	91 $\pm$ 7	94 $\pm$ 5	.024
<b>Sizing</b>				
Valve size/minimal annulus diameter $\times$ 100, %	127 $\pm$ 10	130 $\pm$ 10	121 $\pm$ 8	< .001
Valve size/maximal annulus diameter $\times$ 100, %	101 $\pm$ 8	105 $\pm$ 8	96 $\pm$ 6	< .001
Valve size/mean annulus diameter $\times$ 100, %	112 $\pm$ 8	116 $\pm$ 7	107 $\pm$ 5	< .001
Valve perimeter/perimeter native annulus $\times$ 100	110 $\pm$ 9	114 $\pm$ 7	103 $\pm$ 7	< .001
<b>Depth of implantation</b>				
Noncoronary sinus, mm	7 $\pm$ 4	7 $\pm$ 4	8 $\pm$ 2	.055
Left-coronary sinus, mm	8 $\pm$ 3	8 $\pm$ 4	8 $\pm$ 2	.459
<b>Post-dilatation</b>				
Post implantation balloon dilation	23 (17.2)	15 (17.9)	8 (16.0)	.783
Balloon nominal diameter/mean annulus diameter $\times$ 100, %	102 $\pm$ 8	99 $\pm$ 8	107 $\pm$ 3	.019
Balloon nominal diameter/valve size $\times$ 100, %	92 $\pm$ 8	88 $\pm$ 5	102 $\pm$ 6	< .001
<b>AR post-TAVI</b>				
AR index	23 $\pm$ 9	22 $\pm$ 10	24 $\pm$ 6	.454
AR post TAVI by aortography				
Grade 0	17 (12.7)	4 (4.8)	13 (26.0)	
Grade I	93 (69.4)	58 (69.0)	35 (70.0)	
Grade II	22 (16.4)	20 (23.8)	2 (4.0)	
Grade III	2 (1.5)	2 (2.4)	0 (0.0)	
Grade IV	0 (0.0)	0 (0.0)	0 (0.0)	
Grade $\geq$ II	24 (17.9)	22 (26.2)	2 (4.0)	.001
AR post-TAVI by echocardiography				
Mild (< 10% circumferential extend of the leakage)	93 (80.2)	55 (76.4)	38 (86.4)	
Moderate (10%-29% circumferential extend of the leakage)	19 (16.4)	15 (20.8)	4 (9.1)	
Severe (> 30% circumferential extend of the leakage)	4 (3.4)	2 (2.8)	2 (4.5)	
More than mild ( $\geq$ 10% circumferential extend of the leakage)	23 (19.8)	17 (23.6)	6 (13.6)	.191

AR, aortic regurgitation; ESV, Edwards SAPIEN valve; MCS, Medtronic CoreValve system; TAVI, transcatheter aortic valve implantation. Data are expressed as no. (%) or mean  $\pm$  standard deviation

$D_{max}$ ,  $105 \pm 8$  mm vs  $96 \pm 6$  mm;  $P < .001$ ;  $D_{mean}$ ,  $116 \pm 7$  mm vs  $107 \pm 5$  mm;  $P < .001$ , perimeter  $114 \pm 7$  vs  $103 \pm 7$ ;  $P < .001$ ) (Figure 3). After valve implantation, the depth of implantation was similar between the 2 groups as was the use of post-dilation (MCS, 17.9% vs ESV, 16%;  $P = .783$ ), although the balloon used for post-dilation in the MCS group was smaller relative to the mean diameter of the patient's annulus ( $99 \pm 8$  mm vs  $107 \pm 3$  mm;  $P = .019$ ) and nominal valve size ( $88 \pm 5$  mm vs  $102 \pm 6$  mm;  $P < .001$ ).

Details of the frame geometry of the 2 valves are summarized in Table 3. The degree of expansion of the MCS valve was less at its inflow compared with the ESV ( $83 \pm 7$  vs  $92 \pm 4$ ;  $P < .001$ ). When we related the degree of expansion to the patient's annulus (adjusted expansion), no difference was found between valves either at the inflow or at the nadir/mid-segment (MCS vs ESV,  $0.95 \pm 0.09$  vs  $0.95 \pm 0.05$  and  $0.91 \pm 0.07$  vs  $0.91 \pm 0.06$ , respectively) (Table 3). The MCS valve was more elliptical than the ESV at all levels (inflow,  $82 \pm 8$  vs  $95 \pm 3$ ;  $P < .001$ ; nadir/mid segment,  $83 \pm 8$  vs  $95 \pm 4$ ;  $P < .001$ ; coaptation/outflow,  $90 \pm 6$  vs  $96 \pm 3$ ;  $P < .001$ ). This was also the case for the adjusted eccentricity (MCS,  $4 \pm 13$  vs ESV,  $21 \pm 11$ ;  $P < .001$ ), which was more prevalent after MCS than ESV implantation (MCS, 36% vs 2%  $P < .001$ ) (Figure 4).

Separate analysis for the ESV-XT and ESV-S3 are summarized in Tables 2–5 of the supplementary material. Despite a lesser use of balloon predilation and less oversizing, a higher degree of expansion of the S3 compared with XT was noted and a similar degree of circularity with a trend to less post-dilation.

### Aortic Regurgitation Post-implantation and Before Discharge

By contrast angiography, the prevalence of AR grade 0-1 and 2-4 after MCS implantation was 73.8% and 26.2% and was 96% and 4%, respectively, after ESV implantation. By echocardiography at discharge, the prevalence of no-to-mild and moderate-to-severe AR was 76.4% and 23.6% after MCS implantation and was 86.4% and 13.6% after ESV implantation (Table 2). Table 4 summarizes the relationship between frame geometry and AR post-TAVI (echocardiography at discharge, VARC-2). Aortic regurgitation  $\geq 10\%$  was related to the adjusted degree of expansion (the lesser the expansion, the more AR) as well as with the eccentricity and adjusted eccentricity of the frame at the nadir (MCS)/mid segment (ESV) and coaptation (MCS)/outflow (ESV). A similar trend was seen when we separately analyzed patients who received the MCS or ESV, but the sample size precludes firm conclusions.

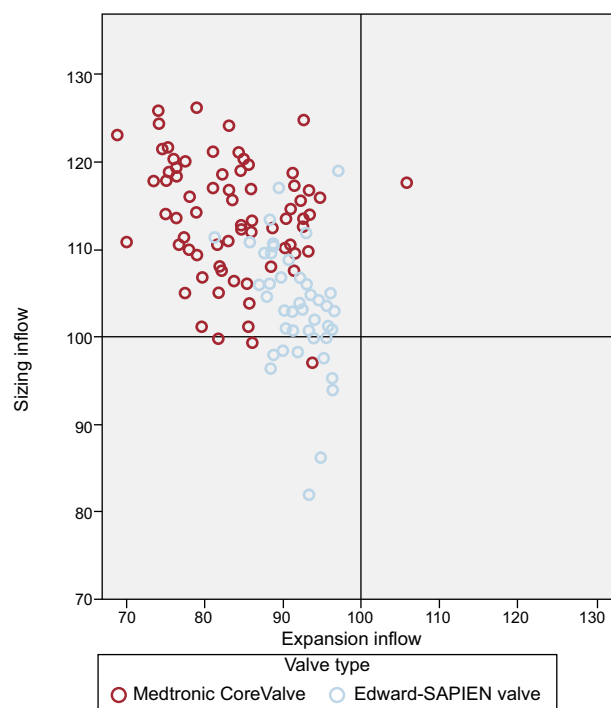


Figure 3. Scatter plot of the relationship between sizing (nominal valve perimeter/perimeter annulus measured by multislice computed tomography  $\times 100$ ) and expansion (perimeter measured valve at the inflow/nominal valve perimeter at the inflow level  $\times 100$ ).

### DISCUSSION

The main finding of the present study is that the frame of the self-expanding MCS valve is less expanded at its inflow and overall is more eccentric than the balloon-expandable ESV. This was also true when eccentricity was corrected for the eccentricity of the patient's annulus, which was found to be associated with a higher prevalence of AR by both angiography and echocardiography. These data indicate the existence of a device-specific device-host interaction that is associated with AR post-TAVI.

We acknowledge that these findings stem from an observational study with limited sample size and uneven distribution of patients per valve in addition to the absence of randomized

Table 3  
Frame Analysis by Rotational Angiography

	Entire cohort (n = 134)	MCS (n = 84)	ESV (n = 50)	P
<i>Degree of expansion</i>				
Degree of valve expansion at the inflow, %	$86 \pm 8$	$83 \pm 7$	$92 \pm 4$	$< .001$
Degree of valve expansion at the nadir/mid segment, %	$89 \pm 3$	$90 \pm 3$	$88 \pm 3$	.001
Degree of valve expansion at the coaptation/outflow, %	$95 \pm 5$	$97 \pm 4$	$92 \pm 4$	$< .001$
Adjusted expansion	$0.95 \pm 0.08$	$0.95 \pm 0.09$	$0.95 \pm 0.05$	.785
<i>Frame eccentricity</i>				
Degree of eccentricity valve at inflow, %	$87 \pm 9$	$82 \pm 8$	$95 \pm 3$	$< .001$
Degree of eccentricity valve at nadir/mid segment, %	$88 \pm 9$	$83 \pm 8$	$95 \pm 4$	$< .001$
Degree of eccentricity valve at coaptation/outflow, %	$92 \pm 6$	$90 \pm 6$	$96 \pm 3$	$< .001$
Degree of eccentricity nadir/mid segment adjusted to eccentricity native annulus	$10 \pm 15$	$4 \pm 13$	$21 \pm 11$	$< .001$
Nadir/mid more eccentric than the native annulus	29 (21.6)	28 (36.4)	1 (2.1)	$< .001$

ESV, Edwards SAPIEN valve; MCS, Medtronic CoreValve system. Data are expressed as no. (%) or mean  $\pm$  standard deviation

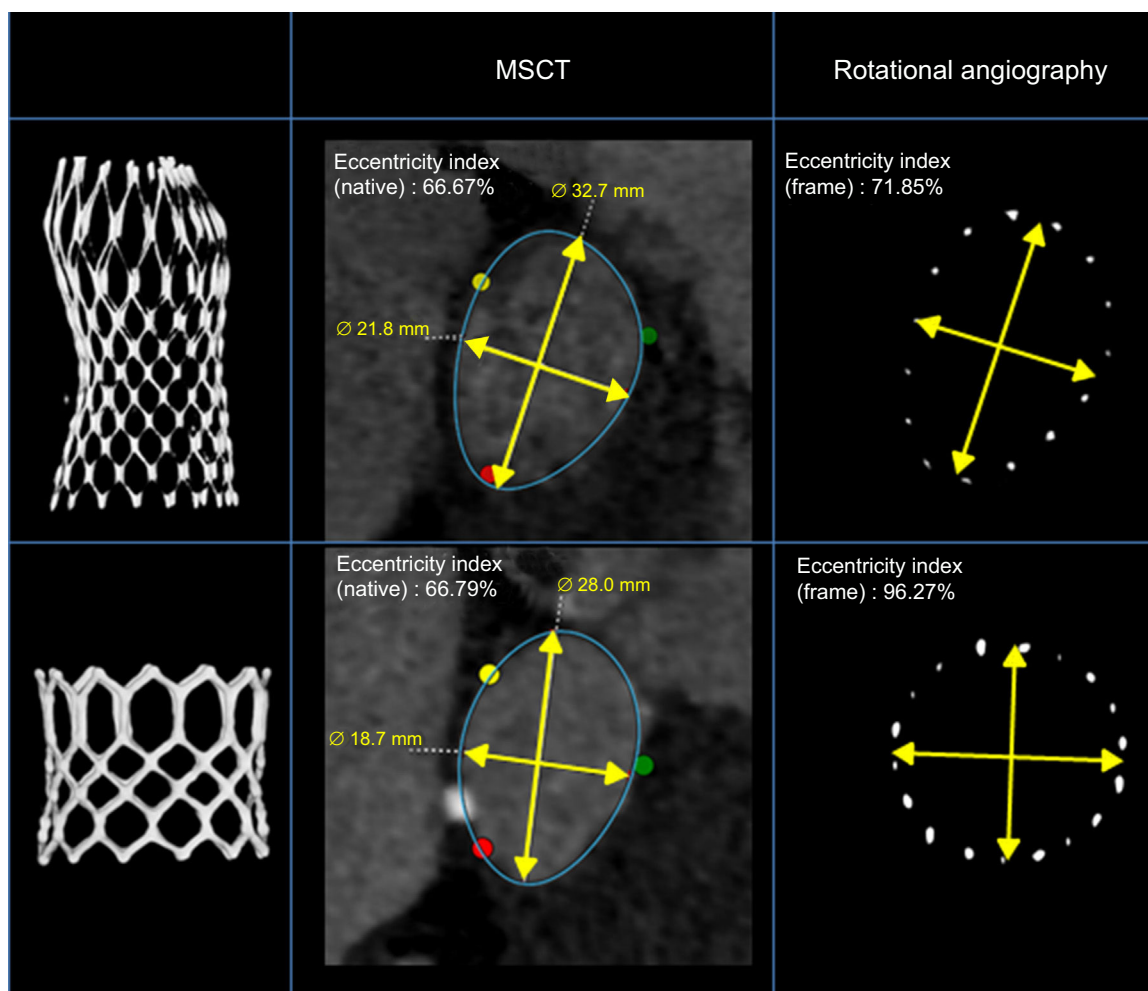


**Figure 4.** Example of the aortic annulus of 2 patients with similar annulus eccentricity (multislice computed tomography) treated with the Medtronic CoreValve and Edwards SAPIEN valve. Left panel: 3-dimensional rendered image of frame implanted. Right panel: frame geometry at the level of the nadir (Medtronic CoreValve) and mid segment (Edwards SAPIEN valve) by rotational angiography post transcatheter aortic valve implantation. Mid panel: cross-sectional view and eccentricity index of the Medtronic CoreValve (above) and Edwards SAPIEN valve (below) post transcatheter aortic valve implantation. MSCT, multislice computed tomography.

allocation to one valve or the other, thereby precluding direct comparison of valve morphology and function. Nevertheless, there were no differences in baseline characteristics, including aortic root anatomy between patients receiving the MCS or ESV valve. Interestingly, balloon dilation before valve implantation was performed more often in patients receiving the MCS valve (albeit with a smaller balloon relative to the patient's annulus) in addition to a higher degree of oversizing (valve size relative to all MSCT-derived measures of the patient's annulus) in comparison with patients treated with the ESV. In addition, we found a higher incidence of  $AR \geq 2$  by angiography after MCS but no difference between the 2 valves when using echocardiography. This may be explained by the intrinsic differences between the 2 techniques for assessing AR in addition to their timing (angiography immediately after TAVI, echocardiography before discharge). In addition, the change may have played a role given the uneven distribution of patients for AR assessment (MCS, 84; ESV, 50).

The current clinical findings in patients with aortic stenosis who underwent TAVI are underscored by the experimental work of Tzamtzis et al.<sup>19</sup> In a study using finite element analysis to study hoop force of the MCS and ESV-XT for different dimensions and rigidity of the left ventricle outflow tract, these authors found that the ESV had a stronger hoop force than the MCS for any left ventricle outflow tract diameter, independently of left ventricle

outflow tract rigidity.<sup>19</sup> This is not surprising since such a biomechanical property is mandatory for the safe implantation of the ESV valve, which is based upon the plastic deformation and, therefore the frame must withstand the forces of recoil of the left ventricle outflow tract after deflation of the delivery balloon, thereby ensuring valve geometry and function. A lesser hoop force of the self-expanding or super-elastic MCS valve is underscored by a clinical observation reporting that aortic root calcification had a higher discriminatory power for the prediction of balloon dilation after MCS valve implantation than annulus dimensions or the prosthesis-to-annulus ratio.<sup>12</sup> Differences in biomechanical properties may also explain the current and previously reported difference in eccentricity between the MCS and ESV valves. In a series of 30 patients, symmetrical expansion of the MCS valve was seen in only 5 patients (17%), while circularity of the ESV was seen in all but 2 out of 89 patients (98%) and was independent of the native annular anatomy.<sup>13,14</sup>

The aggregate of these clinical and experimental data confirm and explain why the MCS frame conforms to the geometry of the patient's annulus, while the ESV dictates the geometry of the annulus and its contribution to the development of AR. Less AR after ESV implantation has consistently been reported by a number of observational studies and 1 randomized clinical trial directly comparing MCS and ESV.<sup>8–10</sup> The question is to what extent does





- patients with severe aortic stenosis at extreme risk for surgery. *J Am Coll Cardiol*. 2014;63:1972–81.
4. Adams DH, Popma JJ, Reardon MJ, Yakubov SJ, Coselli JS, Deeb GM, et al. Transcatheter aortic-valve replacement with a self-expanding prosthesis. *N Engl J Med*. 2014;370:1790–8.
  5. Mylotte D, Osnabrugge RL, Windecker S, Lefèvre T, De Jaegere P, Jeger R, et al. Transcatheter aortic valve replacement in Europe: adoption trends and factors influencing device utilization. *J Am Coll Cardiol*. 2013;62:210–9.
  6. O'Sullivan KE, Gough A, Segurado R, Barry M, Sugrue D, Hurley J. Is valve choice a significant determinant of paravalvular leak post-transcatheter aortic valve implantation? A systematic review and meta-analysis. *Eur J Cardiothorac Surg*. 2014;45:826–33.
  7. Van Belle E, Juthier F, Susen S, Vincetelli A, Iung B, Dallongeville J, et al. Post-procedural aortic regurgitation in balloon-expandable and self-expandable TAVR procedures: analysis of predictors and impact on long-term mortality: insights from the FRANCE2 Registry. *Circulation*. 2014;129:1415–27.
  8. Abdel-Wahab M, Mehili J, Frerker C, Neumann FJ, Kurz T, Tölg R, et al. Comparison of balloon-expandable vs self-expandable valves in patients undergoing transcatheter aortic valve replacement: the CHOICE randomized clinical trial. *JAMA*. 2014;311:1503–14.
  9. Généreux P, Head SJ, Hahn R, Daneault B, Kodali S, Williams MR, et al. Paravalvular leak after transcatheter aortic valve replacement: the new Achilles' heel? A comprehensive review of the literature. *J Am Coll Cardiol*. 2013;61:1125–36.
  10. Athappan G, Patvardhan E, Tuzcu EM, Svensson LG, Lemos PA, Fraccaro C, et al. Incidence, predictors, and outcomes of aortic regurgitation after transcatheter aortic valve replacement: meta-analysis and systematic review of literature. *J Am Coll Cardiol*. 2013;61:1585–95.
  11. Ng AC, Delgado V, Van der Kley F, Shanks M, Van de Veire NR, Bertini M, et al. Comparison of aortic root dimensions and geometries before and after transcatheter aortic valve implantation by 2- and 3-dimensional transesophageal echocardiography and multislice computed tomography. *Circ Cardiovasc Imaging*. 2010;3:94–102.
  12. Schultz C, Rossi A, Van Mieghem N, Van der Boon R, Papadopoulou SL, Van Domburg R, et al. Aortic annulus dimensions and leaflet calcification from contrast MSCT predict the need for balloon post-dilatation after TAVI with the Medtronic CoreValve prosthesis. *EuroIntervention*. 2011;7:564–72.
  13. Schultz CJ, Weustink A, Piazza N, Otten A, Mollet N, Krestin G, et al. Geometry and degree of apposition of the CoreValve ReValving system with multislice computed tomography after implantation in patients with aortic stenosis. *J Am Coll Cardiol*. 2009;54:911–8.
  14. Binder RK, Webb JG, Toggweiler S, Freeman M, Barbanti M, Willson AB, et al. Impact of post-implant SAPIEN XT geometry and position on conduction disturbances, hemodynamic performance, and paravalvular regurgitation. *JACC Cardiovasc Interv*. 2013;6:462–8.
  15. Schultz CJ, Lauritsch G, Van Mieghem N, Rohkohl C, Serruys PW, Van Geuns RJ, et al. Rotational angiography with motion compensation: first-in-man use for the 3D evaluation of transcatheter valve prosthesis. *EuroIntervention*. 2015;11:442–9.
  16. Schultz CJ, Moelker AD, Tzikas A, Rossi A, Van Geuns RJ, De Feyter PJ, et al. Cardiac CT: Necessary for precise sizing for transcatheter aortic implantation. *EuroIntervention*. 2010;6 Suppl G:G6–13.
  17. Sellers RD, Levy MJ, Amplatz K, Lillehey CW. Left retrograde cardioangiography in acquired cardiac disease: technic, indications and interpretations in 700 cases. *Am J Cardiol*. 1964;14:437–47.
  18. Kappetein AP, Head SJ, Généreux P, Piazza N, Van Mieghem NM, Blackstone EH, et al. Updated standardized endpoint definitions for transcatheter aortic valve implantation: the Valve Academic Research Consortium-2 consensus document. *Eur Heart J*. 2012;33:2403–18.
  19. Tzamtzis S, Viquerat J, Yap J, Mullen MJ, Burriesci G. Numerical analysis of the radial force produced by the Medtronic-CoreValve and Edwards-SAPIEN after transcatheter aortic valve implantation (TAVI). *Med Eng Phys*. 2013;35:125–30.
  20. Meredith IT, Walters DL, Dumonteil N, Worthley SG, Tchéhché D, Manoharan G, et al. Transcatheter aortic valve replacement for severe symptomatic aortic stenosis using a repositionable valve system: 30-day primary endpoint results from the REPRISE II study. *J Am Coll Cardiol*. 2014;64:1339–48.
  21. Piazza N, Martucci G, Lachapelle K, De Varennes B, Bilodeau L, Buihieu J, et al. First-in-human experience with the Medtronic CoreValve Evolut R. *EuroIntervention*. 2014;9:1260–3.
  22. Rodríguez-Olivares R, Van Mieghem NM, De Jaegere PP. The role of frame geometry assessment during transcatheter aortic valve replacement by rotational angiography. *JACC Cardiovasc Interv*. 2014;7:e191–2.
  23. García E, Unzué L, García E, Solís J, Teijeiro R, Tarancón B. Experiencia inicial con la válvula aórtica percutánea de muy bajo perfil SAPIEN 3. *Rev Esp Cardiol*. 2014;67:953–4.
  24. Larman Tellechea M, Telleria Arrieta M, Lasa Larraya G, Sanmartin Pena JC, Gaviria Molinero K. Implante transcáteter de la válvula aórtica Lotus™: serie inicial de 5 casos. *Rev Esp Cardiol*. 2014;67:956–8.